

See discussions, stats, and author profiles for this publication at: <https://www.researchgate.net/publication/51432769>

Simplified Protocol for Detection of Protein–Ligand Interactions via Surface–Enhanced Resonance Raman Scattering and Surface–Enhanced Fluorescence

ARTICLE *in* ANALYTICAL CHEMISTRY · SEPTEMBER 2008

Impact Factor: 5.64 · DOI: 10.1021/ac800642g · Source: PubMed

CITATIONS

59

READS

64

7 AUTHORS, INCLUDING:



Yasutaka Kitahama

Kwansei Gakuin University

56 PUBLICATIONS 643 CITATIONS

SEE PROFILE



Bing Zhao

Jilin University

275 PUBLICATIONS 5,011 CITATIONS

SEE PROFILE



Yukihiro Ozaki

Kwansei Gakuin University

916 PUBLICATIONS 17,747 CITATIONS

SEE PROFILE

Simplified Protocol for Detection of Protein–Ligand Interactions via Surface-Enhanced Resonance Raman Scattering and Surface-Enhanced Fluorescence

Xiao X. Han,^{†,*} Yasutaka Kitahama,[‡] Yuhei Tanaka,[‡] Jie Guo,[†] Wei Q. Xu,[†] Bing Zhao,^{*,†} and Yukihiro Ozaki^{*,†}

State Key Laboratory of Supramolecular Structure and Materials, Jilin University, Changchun 130012, P. R. China, and Department of Chemistry, School of Science and Technology, Kwansei Gakuin University, Sanda, Hyogo 669-1337, Japan

A simple and effective protocol for detections of protein–protein and protein–small molecule interactions has been developed. After interactions between proteins and their corresponding ligands, we employed colloidal silver staining for producing active substrates for surface-enhanced Raman scattering (SERS) and surface-enhanced fluorescence (SEF). Tetramethylrhodamine isothiocyanate (TRITC) and Atto610 were used for both Raman and fluorescent probes. We detected interactions between human IgG and TRITC–anti-human IgG, and those between avidin and Atto610–biotin by surface-enhanced resonance Raman scattering (SERRS) and SEF. The detection limits of the proposed SERRS-based method are comparable to those of the proposed SEF-based one, 0.9 pg/mL for anti-human IgG and 0.1 pg/mL for biotin. This protocol exploits several advantages of simplicity over other SERS and SEF-based related methods because of the protein staining-based strategy for silver nanoparticle assembling, high sensitivity from SERRS and SEF, and high stability in photostability comparing to fluorescence-based protein detections. Therefore, the proposed method for detection of protein–ligand interactions has great potential in high-sensitivity and high-throughput chip-based protein function determination.

Proteins are vital parts of living organisms, as they are main components of the physiological metabolic pathways of cells. Protein studies can give a much better understanding of an organism than genomics, so large-scale studies of proteins, called proteomics, have been started for the quest of protein structures and functions.¹ Protein microchips are powerful tools for proteomic research, and they allow researchers to study proteins on a grand scale.^{2,3} The purpose of functional protein arrays is to quickly probe the activity of a given protein against many targets

simultaneously, and they are usually used to identify protein–protein interactions, substrates of protein kinases, targets of biologically active small molecules.⁴ The current preferred detection method for functional protein arrays is fluorescence, which is safer than radiolabeling. However, for fluorescence-based detection, broad emission spectra displayed by molecular fluorophores make it incapable of multiplexing, and the drawback of susceptibility to photobleaching may greatly weaken its detection limit.

As an ultrasensitive spectroscopic technique,^{5–14} surface-enhanced resonance Raman scattering (SERRS) has achieved a level of single-molecule detection under favorable circumstances. Recently, many surface-enhanced Raman scattering (SERS) or SERRS based high-sensitivity molecular sensing platforms, especially biomolecular sensing, have been successfully created.^{15–22} In many SERS or SERRS-based approaches for protein detections,

- (4) Zhu, H.; Snyder, M. *Curr. Opin. Chem. Biol.* **2003**, *1*, 55–63.
- (5) Jeanmaire, D. L.; Van Duyne, P. R. *J. Electroanal. Chem.* **1977**, *84*, 1–20.
- (6) Chang, R. K.; Furtak, T. E., Eds. *Surface-Enhanced Raman Scattering*; Plenum Press: New York, 1982.
- (7) Moskovits, M. *Rev. Mod. Phys.* **1985**, *57*, 783–825.
- (8) Kerker, M., Eds. *Selected Papers on Surface-Enhanced Raman Scattering*; SPIE: Bellingham, WA, 1990.
- (9) Kneipp, K.; Kneipp, H.; Itzkan, I.; Dasari, R. R.; Feld, M. S. *Chem. Rev.* **1999**, *99*, 2957–2975.
- (10) Smith, W. E.; Rodger, C. *Handbook of Vibrational Spectroscopy Vol. 1: Theory and Instrumentation*; Chalmers, J. M., Griffiths, P. R., Eds.; John Wiley & Sons Ltd: Chichester, U.K., 2002; pp 775–784.
- (11) Schatz, G. C.; Van Duyne, P. R. *Handbook of Vibrational Spectroscopy Vol. 1: Electromagnetic Mechanism of Surface-Enhanced Spectroscopy*, Chalmers, J. M., Griffiths, P. R., Eds.; John Wiley & Sons Ltd.: Chichester, U.K., 2002; pp 759–774.
- (12) Cao, Y. W. C.; Jin, R. C.; Mirkin, C. A. *Science* **2002**, *297*, 1536–1540.
- (13) Aroca, R. *Surface-Enhanced Vibrational Spectroscopy*; John Wiley & Sons Ltd.: Chichester, U.K., 2006; pp 141–176.
- (14) Kneipp, K.; Moskovits, M.; Kneipp, H., Eds. *Surface-Enhanced Raman Scattering-Physics and Applications*; Springer: Heidelberg and Berlin, 2006.
- (15) Cao, Y. C.; Jin, R.; Nam, J. M.; Thaxton, C. S.; Mirkin, C. A. *J. Am. Chem. Soc.* **2003**, *125*, 14676–14677.
- (16) Xu, S. P.; Ji, X. H.; Xu, W. Q.; Li, X. L.; Wang, L. Y.; Bai, Y. B.; Zhao, B.; Ozaki, Y. *Analyst* **2004**, *129*, 63–68.
- (17) Maniaran, M.; Jana, N. R. *J. Raman Spectrosc.* **2007**, *38*, 1326–1331.
- (18) Ni, J.; Lipert, R. J.; Dawson, G. B.; Porter, M. D. *Anal. Chem.* **1999**, *71*, 4903–4908.
- (19) Grubisha, D. S.; Lipert, R. J.; Park, H. Y.; Driskell, J.; Porter, M. D. *Anal. Chem.* **2003**, *75*, 5936–5943.
- (20) Mulvaney, S. P.; Musick, M. D.; Keating, C. D.; Natan, M. J. *Langmuir* **2003**, *19*, 4784–4790.

* To whom correspondence should be addressed. E-mail: ozaki@kwansei.ac.jp.

[†] Jilin University.

[‡] Kwansei Gakuin University.

(1) Twyman, R. M. *Principles of Proteomics*; BIOS Scientific Publishers: New York; 2004.

(2) Blackstock, W. P.; Weir, M. P. *Trends Biotechnol.* **1999**, *17*, 121–127.

(3) MacBeath, G.; Schreiber, S. L. *Science* **2000**, *289*, 1760–1763.

SERS is employed to determine protein–ligand interactions by using Raman dye-labeled gold or silver nanoparticle probes, and these probes hold the advantages of high-sensitivity and high-selectivity. However, the complex synthesis procedure of nanoparticle probes may restrict their applications to high-throughput chip-based protein detections.

Raman signal can be enhanced due to the effect of resonance Raman enhancement, and it can be further strengthened through surface enhancement, which is called SERRS. SERRS usually emerges among other surface-enhanced phenomena (e.g., surface-enhanced absorption, surface-enhanced fluorescence (SEF)). SEF yields an overall improvement in the fluorescence detection efficiency through modification and control of the local electromagnetic environment of the emitter.²³ Metal-enhanced fluorescence is a phenomenon where the quantum yield and photostability of weakly fluorescent molecules are dramatically increased, and it has been proved to be able to significantly improve the sensitivity of fluorescence.^{24,25} Metal-enhanced fluorescence is becoming a powerful tool for the fluorescence-based applications of high-throughput screening, immunoassays and protein–protein detections.^{26,27} Many quartz or glass substrates with deposited metal nanostructures have been prepared for SEF studies, for example, silver island films, colloidal nanocrystals or metal clusters.^{23–27}

In conventional SERS-based studies, SERS-active substrates are usually first prepared (e.g., metal colloid, electrodes, or island films), and then analytes are assembled on these substrates for further SERS detections. For most SERS-based protein detections on chips, antibodies and probes are usually linked to metal nanoparticles. In our studies, we use a contrary way, which is based on strong interactions between proteins and silver nanoparticles.²⁸ After interactions between proteins and target analytes, we obtain SERS-active substrates (silver aggregates) by using colloidal silver staining for total proteins. Thus, compared to the metal nanoparticle probe-based ones, our method can prevent binding sites of target analytes (especially those contain sulfhydryl groups) from destruction by metal nanoparticles. Moreover, colloidal silver staining for proteins is a much simpler way to obtain SERS-active substrates than those nanoparticle probe-based methods. Furthermore, for the first time we observed SEF on the proposed SERS-active substrates.

In this way, we can determine protein–ligand interactions by SERRS or SEF of labels that are linked to target analytes. The

same instrument is used for observing both images and spectra of fluorescence emission and Raman scattering. The present method has great potential particularly for functional protein assays because of the simplified procedure of SERRS or SEF-active substrate assembling, high sensitivity of SERRS and SEF, and photostability over fluorescence-based methods. Moreover, we find that the proposed SERRS-based method is more stable than the proposed SEF-based one in photostability, while the detection limit is comparable.

EXPERIMENTAL SECTION

Biochemicals and Chemicals. Human IgG (I4506), avidin (A9275), TRITC–anti-human IgG (Fc specific, T4530), and Atto 610–biotin (43292) were purchased from Sigma Co., Ltd., and used without further purification. (3-Aminopropyl)trimethoxysilane, glutaraldehyde and Tween 20 were obtained from Sigma-Aldrich. Bovine serum albumin (BSA), silver nitrate, trisodium citrate and all other chemicals were purchased from Wako Co., Ltd. Triply distilled water was used throughout the present study.

Buffers. The phosphate-buffered saline (PBS; 0.01 M, pH 7.2) used in the present study contained 0.8% NaCl, 0.02% KH_2PO_4 , 0.02% KCl and 0.12% $\text{Na}_2\text{HPO}_4 \cdot 12\text{H}_2\text{O}$. A blocking buffer was prepared by dissolving BSA in the PBS buffer (containing 1% BSA). A washing buffer was prepared by adding Tween-20 to the PBS buffer (containing 0.05% Tween 20).

Preparation of Silver Colloid. Colloidal silver was prepared by the aqueous reduction of silver nitrate (10^{-3} M, 200 mL) with trisodium citrate (1%, 4 mL) using a method of Lee and Meisel.²⁹ The plasmon absorption maximum of the silver colloid we prepared was located at 415 nm.

Protocol of Protein–Ligand Interactions. (i) Functionalization of Glass Slides.³⁰ Glass slides were cleaned by immersing them in a boiling solution prepared by mixing 30% H_2O_2 and 98% H_2SO_4 with a volume ratio of 3:7. After cooling, the slides were rinsed repeatedly with triply distilled water. The glass slides with hydroxyl surfaces were soaked in a 2% (3-aminopropyl)trimethoxysilane solution for 30 min, then rinsed by ethanol and dried under a stream of nitrogen. Finally, silanized glass slides were immersed in a 2.5% glutaraldehyde solution for 2 h. After that, the aldehyde-functionalized glass slides were rinsed by the PBS buffer (pH 7.2) for three times.

(ii) Protein–Ligand Interactions. Human IgG (100 $\mu\text{g}/\text{mL}$ in the 0.01 M PBS buffer) and avidin (40 $\mu\text{g}/\text{mL}$ in the 0.01 M PBS buffer) were immobilized on the aldehyde-functionalized glass slides by immersing the slides in the two protein solutions for 2 h at 37 °C, respectively. After having been rinsed three times with a washing buffer, the glass slides were soaked in a blocking buffer for 2 h at 37 °C, and then rinsed again three times with a washing buffer. The glass slides coated with human IgG and avidin were immersed in the solutions of their corresponding ligands TRITC–anti-human IgG (Fc specific) and Atto610–biotin for one hour at 37 °C. Then all the glass slides were rinsed three times by a washing buffer.

Colloidal Silver Staining. After specific-binding interactions, the glass slides were soaked in a freshly prepared silver colloid

- (21) Driskell, J. D.; Uhlenkamp, J. M.; Lipert, R. J.; Porter, M. D. *Anal. Chem.* **2007**, *79*, 4141–4148.
- (22) Gong, J. L.; Liang, Y.; Huang, Y.; Chen, J. W.; Jiang, J. H.; Shen, G. L.; Yu, R. Q. *Biosens. Bioelectron.* **2007**, *22*, 1501–1507.
- (23) Pompa, P. P.; Martiradonna, L.; Torre, A. D.; Sala, F. D.; Manna, L.; Vittorio, M. D.; Calabi, F.; Cingolani, R.; Rinaldi, R. *Nat. Biotechnol.* **2006**, *1*, 126–130.
- (24) Aslan, K.; Holleya, P.; Geddes, C. D. *J. Mater. Chem.* **2006**, *16*, 2846–2852.
- (25) Fort, E.; Gresillon, S. *J. Phys. D: Appl. Phys.* **2008**, *41*, 013001.
- (26) Geddes, C. D.; Aslan, K.; Gryczynski, I.; Malicka, J.; Lakowicz, J. R. In *Review Chapter for Annual Reviews in Fluorescence 2004*; Geddes, C. D., Lakowicz, J. R. Kluwer Academic/Plenum Publishers: New York, 2004; pp 365–401.
- (27) Sauer, U.; Preininger, C.; Krumpel, G.; Stelzer, N.; Kern, W. *Sens. Actuators, B* **2005**, *107*, 178–183.
- (28) (a) Han, X. X.; Jia, H. Y.; Wang, Y. F.; Lu, Z. C.; Wang, C. X.; Xu, W. Q.; Zhao, B.; Ozaki, Y. *Anal. Chem.* **2008**, *80*, 2799–2804. (b) Han, X. X.; Cai, L. J.; Guo, J.; Wang, C. X.; Ruan, W. D.; Han, W. Y.; Xu, W. Q.; Zhao, B.; Ozaki, Y. *Anal. Chem.* **2008**, *80*, 3020–3024.

- (29) Lee, P. V.; Meisel, D. *J. Phys. Chem.* **1982**, *86*, 3391–3395.
- (30) Yoshioka, M.; Mukai, Y.; Matsui, T.; Udagawa, A.; Funakubo, H. *J. Chromatogr.* **1991**, *566*, 361–368.

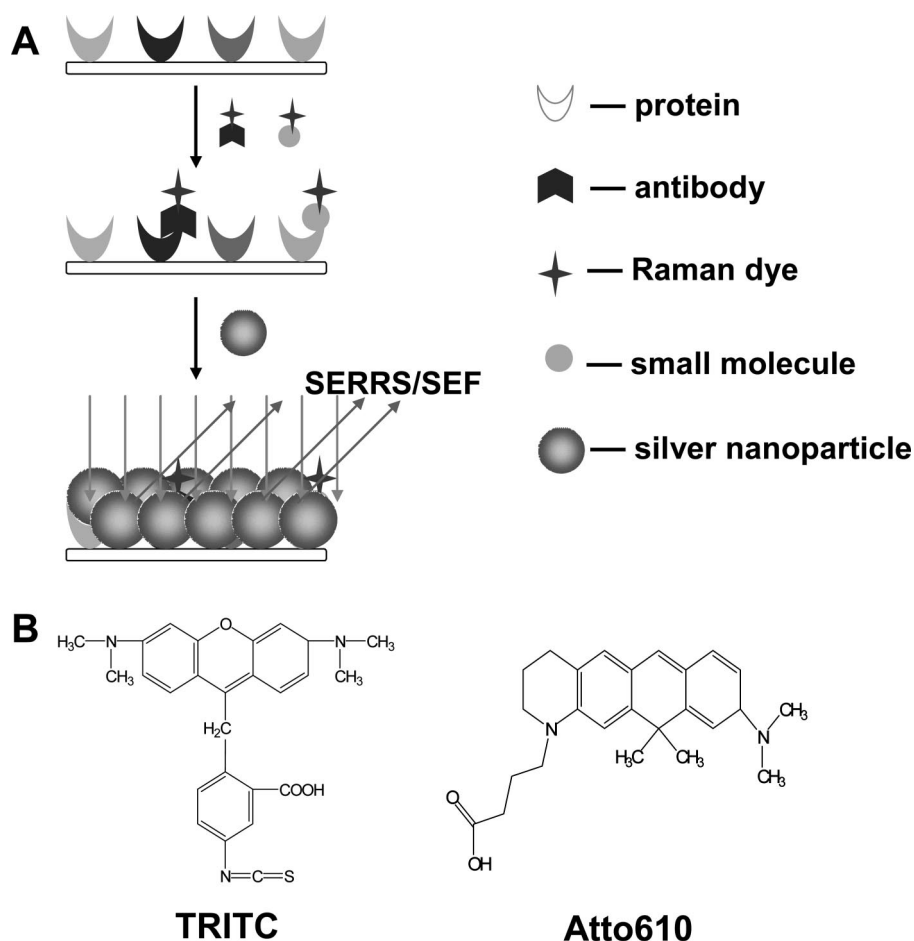


Figure 1. (A) Schematic depiction of the proposed protocol for protein–ligand detections. (B) Chemical structures of TRITC and Atto610.

for 2 h at 37 °C, and then washed by using a washing buffer followed by triply distilled water for three times.

SERRS and SEF Measurements. All fluorescence and SERRS (both images and spectra) were obtained by using the same instrument reported elsewhere.^{31,32} The laser line was delivered through a 45° angle to the stage of an inverted Olympus (Tokyo, Japan) IX70 microscope. Magnification of 60× was employed for all the spectral measurements. Excitation lasers used were an Ar ion laser (2016-05, Spectra Physics, Tokyo) for the 514.5 nm line and a Kr ion laser (643R-AP-A01, Melles Griot, Tokyo) for the 568 nm line. The scattered signal was notch-filtered (Kaiser, Ann Arbor, MI) and directed to the spectrometer (Pro-275, Acton Research Corporation, Acton, MA) for spectra or to a Nikon (Tokyo, Japan) Coolpix5000 digital camera for images. Raman and fluorescence images were recorded with 8 s exposure time. The laser power was 20 mW for the 514.5 nm line and 10 mW for the 568 nm line, and the irradiated sample area was about 700 μm². An Andor (Belfast, U.K.) DV434-FI charge coupled device (CCD) camera in the single-frame mode was used for collecting Raman and fluorescence spectra.

RESULTS AND DISCUSSION

Figure 1A depicts the main procedure of the proposed protocol for protein–ligand binding detections. Glass slides are treated with

silane and aldehyde reagents³⁰ for Schiff's base linkages between aldehyde and amines of proteins. These aldehyde-functionalized glass slides are coated with certain proteins, and then a blocking buffer is used to block the area where there is no nonspecific protein adsorbing on the glass surface. After that, fluorescence-labeled antibodies or small molecules are added for specific interactions, and the bound and free antibodies are separated by a washing step to remove the adsorptions nonspecifically. Colloidal silver staining is used for total proteins after specific interactions. Finally, one can detect protein–protein and protein–small molecule interactions on the silver aggregates by SERRS or SEF images and spectra of the reporters.

Both TRITC and Atto610 are used as Raman and fluorescence reporters for determinations of the interaction between human IgG and TRITC–anti-human IgG (Fc specific) and that between avidin and Atto 610-biotin. TRITC is a derivative of rhodamine, which is a commonly used fluorescein with the maximum absorption of 555 nm and the maximum emission of 580 nm. It is typically conjugated to a protein via primary amines. Atto610, with the maximum absorption of 610 nm, belongs to a new generation of fluorescent labels for the red spectral region of 630 nm with high molecular absorption and quantum yield. Biotin conjugates coupled to Atto610 are very useful for the determination of biotin-binding sites. The structures of the two fluorescent molecules are shown in Figure 1B.

SERRS and SEF Images. Figure 2 shows fluorescence images of TRITC and Atto610 molecules after the interactions

(31) Itoh, T.; Hashimoto, K.; Ozaki, Y. *Appl. Phys. Lett.* **2003**, *83*, 5557–5559.
 (32) Itoh, T.; Hashimoto, K.; Ikehata, A.; Ozaki, Y. *Chem. Phys. Lett.* **2004**, *389*, 225–229.





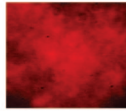
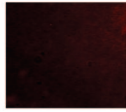
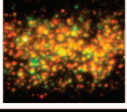
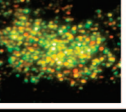
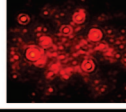
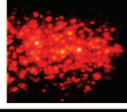
| Dyes (Laser) | TRITC 514.5nm  | | Atto610 568nm  | |
|-------------------------------|--|---|--|---|
| Concentration | 9 μ g/mL | 0.9 ng/mL | 1 μ g/mL | 1 ng/mL |
| Fluorescence (— 5 μ m) |  |  |  |  |
| SERRS/SEF (— 5 μ m) |  |  |  |  |

Figure 2. Fluorescence, SERRS and SEF images of TRITC and Atto610 for different concentrations of target analytes.

between the proteins and their corresponding target analytes, and their SERRS and SEF images after the colloidal silver staining. In the SERRS or SEF images, we can observe many spheroidal silver aggregates with the diameter between 200 and 600 nm after the colloidal silver staining, which originate from the interactions (i.e., hydrophobic, electrostatic and covalent interactions) between the silver nanoparticles and the proteins. Moreover, salts and surfactants in the washing buffer may also have contributions to the formation of aggregates of silver nanoparticles.^{33–35} Comparing the fluorescence and SEF images of the two reporters, we find that, after the adsorption of silver nanoparticles, one can observe relatively stable images of SEF within several minutes, while without silver nanoparticles, the original fluorescence images cannot be observed 30 s after exposing the samples to the corresponding lasers because of photobleaching. It indicates that the presence of silver nanoparticles can enhance the photostability of fluorescent molecules.²⁴

According to distance-dependent enhancement of SERS and SEF, efficient SERS requires close contact of the studied molecules with the metallic surface, a distance below 2–3 nm. However, in close proximity, up to 5 nm, fluorophore emission is strongly quenched primarily by energy transfer to the metal surface, and there is reasonable agreement that the maximal enhancement occurs about 10 nm from the surface.^{36,37} We can find both SERRS and SEF-active silver aggregates after the adsorption of silver nanoparticles in the bottom images of Figure 2. It is very likely that some fluorescent labels which are very close to silver nanoparticles (<5 nm) are quenched, and some others, relatively farther (between 5 and 20 nm) from silver surfaces because of three-dimensional protein structure, are enhanced to a different degree.

Note that the SERRS and SEF images of each fluorescent molecule show significant dependence on the concentrations of target analytes (shown in the bottom of Figure 2). For the concentrated analytes, above 9 ng/mL TRITC–anti-human IgG and 10 ng/mL Atto610-biotin, the SERRS and SEF images show similar color to the fluorescence images, yellow for TRITC and

red for Atto610. For the diluted analytes, below the concentrations of 0.9 ng/mL for TRITC–anti-human IgG and 1 ng/mL for Atto610-biotin, the color of the images changed to green for TRITC and to orange for Atto610. The blue-shifts show increase of SERRS, which appear near the excitation wavelength. From the changes in the SEF and SERRS images we find that SEF is reduced remarkably with the decrease in the concentrations of target analytes, and at the same time, obvious SERRS-active silver aggregates emerge with less covering by SEF-active ones at the same concentrations.

Moreover, we have found that, for both TRITC and Atto610, SERRS images observed with the naked eye are much more stable than fluorescent ones that tend toward photobleaching. We can observe stable SERS-active silver aggregates even at much lower concentration when there are few SEF-active silver aggregates. This indicates the great potential of SERRS images in ultrasensitive determinations of protein–ligand interactions.

SERRS Spectra. To confirm the stability of SERRS, we measured time-dependent SERRS spectra of the two fluorescent labels, since we had observed the stable SERRS images with the naked eye. Figure 3 shows the time-dependent SERRS spectra of TRITC–labeled immunocomplex and Atto610-labeled complex from two SERRS-active single nanoaggregates. It is noted that the SERRS bands of the two complexes yield fairly smooth variations in the intensities and positions within several minutes, which is consistent with the results of previous studies on SERRS of rhodamine 6G.³⁸

Figure 4 depicts time-dependent variations in the intensities of two selected peaks of TRITC (1660 cm^{-1}) and Atto610 (1090 cm^{-1}) at the target concentrations of 0.9 ng/mL and 0.1 ng/mL, respectively. The histograms were built up by the average traces from five different single nanoaggregates. Here, for the first time, Atto610 is used as a SERRS probe for the detection of protein–small molecule interactions. Figure 3B and Figure 4B have confirmed its great potential in SERRS-based studies of protein detections.

Furthermore, we investigated the detection limit of the proposed SERRS-based measurement. The detection limits of 0.9 pg/mL for TRITC–anti-human IgG and 0.1 pg/mL for Atto610-biotin have been achieved, which show the great preponderance of SERRS in high-sensitivity protein detections. (Supporting Information Figure 1)

SEF Spectra. In our experimental conditions, we observed remarkably enhanced fluorescence at lower concentrations of

(33) Pieczonka, N. P. W.; Goulet, P. J. G.; Aroca, R. F. *J. Am. Chem. Soc.* **2006**, *128*, 12626–12627.

(34) Li, X. L.; Zhang, J. H.; Xu, W. Q.; Jia, H. Y.; Wang, X.; Yang, B.; Zhao, B.; Li, B. F.; Ozaki, Y. *Langmuir* **2003**, *19*, 4285–4290.

(35) Hu, J. W.; Zhao, B.; Xu, W. Q.; Fan, Y. G.; Li, B. F.; Ozaki, Y. *Langmuir* **2002**, *18*, 6839–6844.

(36) Lakowicz, J. R.; Geddes, C. D.; Gryczynski, I.; Malicka, J.; Gryczynski, Z.; Aslan, K.; Lukomska, J. *J. Fluoresc.* **2004**, *14*, 425–441.

(37) Geddes, C. D.; Lakowicz, J. R. *J. Fluoresc.* **2002**, *12*, 121–129.

(38) Sasic, S.; Itoh, T.; Ozaki, Y. *J. Raman Spectrosc.* **2005**, *36*, 593–599.

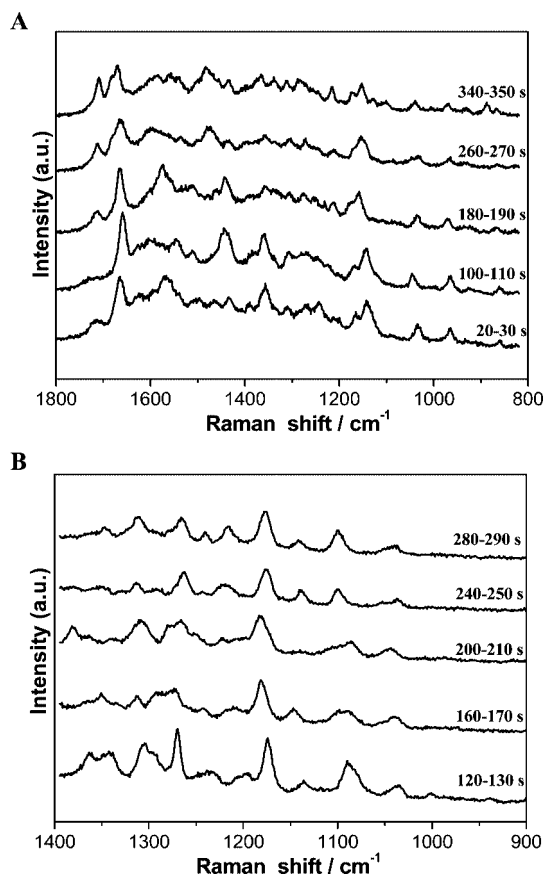


Figure 3. Time-dependent SERRS spectra of (A) TRITC-labeled immunocomplex (0.9 ng/mL TRITC-anti-human IgG) with 514.5 nm laser excitation and (B) Atto610-labeled biotin/avidin complex (0.1 ng/mL Atto610-biotin) with 568 nm laser excitation.

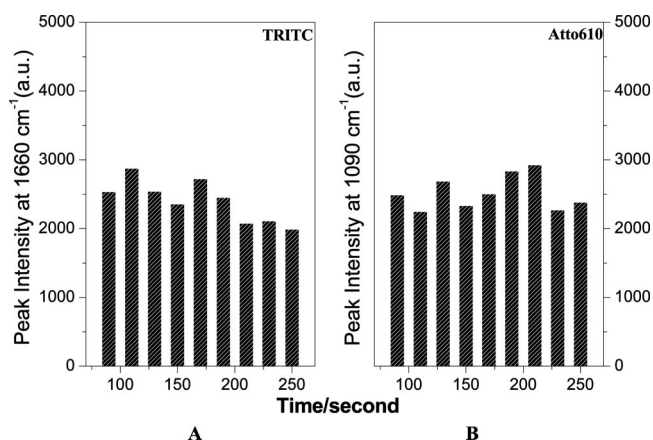


Figure 4. Time-dependent SERRS intensity variations of (A) TRITC-labeled immunocomplex at 1660 cm^{-1} (0.9 ng/mL TRITC-anti-human IgG) and (B) Atto610-labeled biotin/avidin complex at 1090 cm^{-1} (0.1 ng/mL Atto610-biotin). Each histogram was built up by the average intensity of five bands at five different locations on the corresponding sample.

target analytes after the colloidal silver staining. For the TRITC-labeled immunoreactions, above the concentration of $0.9\text{ }\mu\text{g/mL}$, we observed no obvious enhanced fluorescence, which is probably due to the self-quenching of fluorescent molecules. The intensity of fluorescence is enhanced below the concentration of 90 ng/mL with the degree of modification.

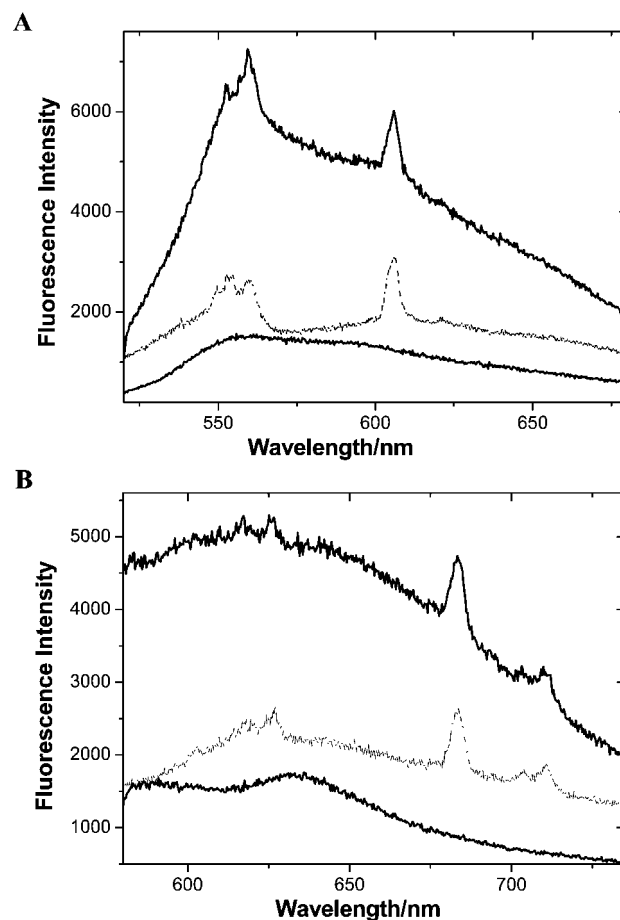


Figure 5. Fluorescence and SEF spectra of (A) TRITC-labeled immunocomplex (0.9 ng/mL TRITC-anti-human IgG) with 514.5 nm laser excitation and (B) Atto610-labeled biotin/avidin complex (1 ng/mL Atto610-biotin) with 568 nm laser excitation. The top, middle, and bottom curves show SEF, SEF after exposing the samples to excitation laser beams for one minute at the same locations as the top curves, and fluorescence without silver nanoparticles, respectively.

Figure 5 depicts fluorescence (the bottom spectrum) and SEF (the top spectrum) of TRITC-labeled immunocomplex with the concentration of TRITC-anti-human IgG of 0.9 ng/mL . By using the same laser power, significantly stronger fluorescence from silver aggregates is observed (shown in the top spectrum of Figure 5), and on average, the fluorescence intensity is about 4-fold enhanced compared with the bottom spectrum. We can find the enhanced integrated intensities of TRITC on silver aggregates within one minute (shown in Figure 6A), which is the reason why we can observe relatively stable SEF image in the bottom of Figure 2.

As for the Atto610-labeled system, we also observed enhanced fluorescence below 10 ng/mL . Figure 5B shows fluorescence (the bottom spectrum) and SEF (the top spectrum) of Atto610-labeled biotin/avidin complex with 1 ng/mL Atto610-biotin. The intensity is strengthened by about 3-fold compared with its fluorescence spectrum. Figure 6B shows time-dependent SEF and fluorescence intensities of Atto610. Though the SEF intensities of TRITC and Atto610 are reduced remarkably after exposing the samples to excitation laser beam for 30 s, the average intensity of fluorescence is significantly enhanced during the measurement time. This

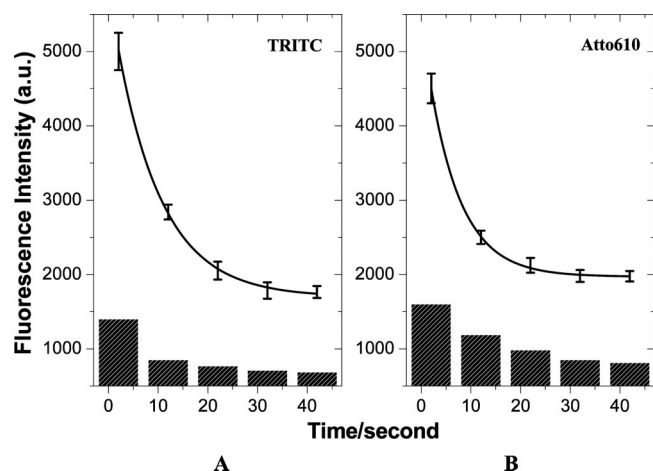


Figure 6. Time-dependent fluorescence and SEF intensities of (A) TRITC-labeled immunocomplex (0.9 ng/mL TRITC-anti-human IgG) measured with 514.5 nm laser excitation, and (B) Atto610-labeled biotin/avidin complex (1 ng/mL Atto610-biotin) measured with 568 nm laser excitation. The curves show the SEF, and the columns show fluorescence without silver nanoparticles. Each error bar and column indicates 5 measurements.

indicates that the present method can improve both detection limits and photostability of fluorescent reporters.

The dashed lines in Figure 6 show the reduced intensities of SEF spectra of TRITC and Atto610 after exposing the samples to the excitation laser line for one minute. Note that the relatively stable SERRS spectra appear on the SEF spectra, which are consistent with the results we obtained in Figure 4.

The detection limit of the proposed SEF-based measurement is as low as 0.1 pg/mL for Atto610-biotin, which is comparable to the proposed SERRS-based one. However, unlike SERRS, this SEF-based method is incapable of yielding stable spectral intensities (Supporting Information Figure 2).

CONCLUSION

In this paper, we have demonstrated a novel simplified SERS and SEF based protocol for detections of protein-ligand interac-

tions. Silver nanoparticles were assembled to the protein-ligand complexes via covalent and noncovalent binding, resulting in the formation of SERS-active silver aggregates. In this way, we have been able to determine protein-protein and protein-small molecule interactions by SERRS and SEF of two fluorescent reporters. From the results, we have found that the sensitivity and photostability of fluorescence-based protein detection can be remarkably improved by the proposed SEF under low concentrations. Moreover, because of the elimination of self-quenching between chromophores and photobleaching, SERRS can compensate for disadvantages of fluorescence in photostability with comparable detection limit, which allows its potential application especially to ultrasensitive assays.

ACKNOWLEDGMENT

This study was supported by the National Natural Science Foundation (Grants 20473029, 20573041, 20773044) of P. R. China; by the Program for Changjiang Scholars and Innovative Research Team in University (IRT0422), Program for New Century Excellent Talents in University, the 111 project (B06009), the Development Program of the Science and Technology of Jilin Province (20060902-02). We also thank China Scholarship Council for their fund support. This work was also supported by KAKENHI (Grant-in-Aid for Scientific Research) on Priority Area "Strong Photon-Molecule Coupling Fields (470, 20043032)" from the Ministry of Education, Culture, Sports, Science and Technology of Japan.

SUPPORTING INFORMATION AVAILABLE

Detection limits of the present method for TRITC-anti-human IgG and Atto610-biotin. This material is available free of charge via the Internet at <http://pubs.acs.org>.

Received for review March 31, 2008. Accepted June 25, 2008.

AC800642G